Rapid #: -16477372

Recent Progresses in the Investigation of
Rare-earth Boron Inverse Sandwich Clusters

LI Wan-Lu[a]　　CHEN Teng-Teng[b]　　JIANG Zhi-Yu[a]

WANG Lai-Sheng [b]②　　LI Jun[a, c] ②

[a] (*Department of Chemistry and Key Laboratory of Organic Optoelectronics & Molecular*

Engineering of Ministry of Education, Tsinghua University, Beijing 100084*, China*)

[b] (*Department of Chemistry, Brown University, Providence, Rhode Island* 02912*, USA*)

[c] (*Department of Chemistry, Southern University of Science and Technology, Shenzhen* 518055*, China*)

ABSTRACT While rare-earth borides represent a class of important materials in modern industries, there are few fundamental researches on their electronic structures and physicochemical properties. Recently, we have performed combined experimental and theoretical studies on rare-earth boron clusters and their cluster-assembled complexes, revealing a series of rare-earth inverse sandwich clusters with fascinating electronic structures and chemical bonding patterns. In this overview article, we summarize recent progresses in this area and provide a perspective view on the future development of rare-earth boride clusters. Understanding the electronic structures of these clusters helps to design materials of *f*-element (lanthanide and actinide) borides with critical physiochemical properties.

Keyword: rare-earth boron clusters, inverse sandwich cluster compounds, *f*-element boride,

bonding of rare-earth compounds; DOI: 10.14102/j.cnki.0254‑5861.2011‑2891

1 INTRODUCTION

Boron, the left neighbor of carbon in the periodic table, is well-known for its electron efficiency. While extensive investigations were performed on carbon-based clusters and materials such as fullerenes, carbon-nanotubes, graphene and graphdiyne, pure boron clusters have been relatively less studied until about two decades ago[1]. We found in 2003 that boron clusters display analogous geometric and electronic structures (e.g. planarity, aromaticity and anti-aromaticity) with hydrocarbon rings[2]. A series of new boron clusters have been characterized by joint photoelectron spectroscopy (PES) and theoretical studies in the past decade. Fascinating electronic structures are found for these electron-deficient clusters featuring multi-center delocalized bonding as well as σ and π aromaticity[3-11]. The discovery of planar or quasi-planar B_{36}^- and B_{35}^- clusters provides the first experimental viability of two-dimensional boron monolayers[12, 13], which we named as borophene akin to graphene. Borophene materials have been recently synthesized experimentally by several groups[14, 15]. The recent experimental observation and computational confirmation of cage-like B_{40}^- and B_{39}^- clusters also represent a milestone of boron clusters, which leads to the identification of a new class of boron structures that we named as borospherene akin to fullerenes[16, 17].

Among various structures of boron clusters, the ring structures are especially unique. The size of the boron monocyclic rings increases from B_3 to B_{10} (Fig. 1), which makes B_7, B_8 and B_9 particularly fit for forming inverse sandwich compounds with large size metal ions[18-23]. Inasmuch as the much higher orbital energies of boron 2*s* and 2*p* orbitals than those of carbon, nitrogen, oxygen and fluorine, boron clusters are especially interesting for binding electropositive metals with high-lying orbitals. As a result, rare-earth borides are ubiquitous as stable solid state compounds[24-29].
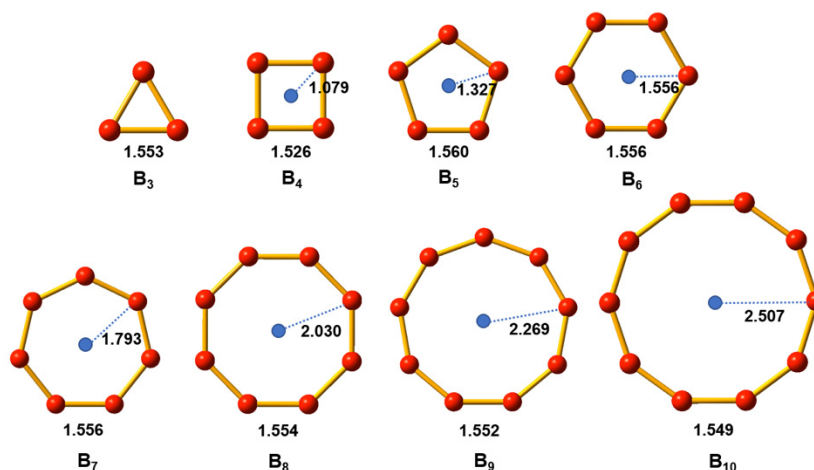
Fig. 1. Size of monocyclic B$_n$ rings with perfect D$_{nh}$ symmetry. Structures are optimized by PBE/TZ2P with ADF program

Among the rare earth elements, lanthanide elements (Ln = La, Lu) feature high-energy *5d* orbitals for weak yet non-negligible covalent orbital overlap with ligands, while the highly radially contracted 4*f* orbitals (Fig. 2) are available for preserving electrons that are often key for magnetic, optical and catalytic applications[30-33]. This peculiarity of extremely contracted 4*f* orbitals (~0.4 Å for La and 0.25 Å for Lu) arises from the *quantum primogenic effect*[34-36], which refers to the fact that the first-shell, nodeless atomic orbitals of each angular quantum number (i.e., 1*s*, 2*p*, 3*d*, 4*f*, 5*g*, ...) tend to be rather contracted in radial distribution due to lack of Pauli repulsion from any inner orbitals with the same angular momentum. These features make lanthanide borides a class of highly intriguing materials for practical applications[27-29].
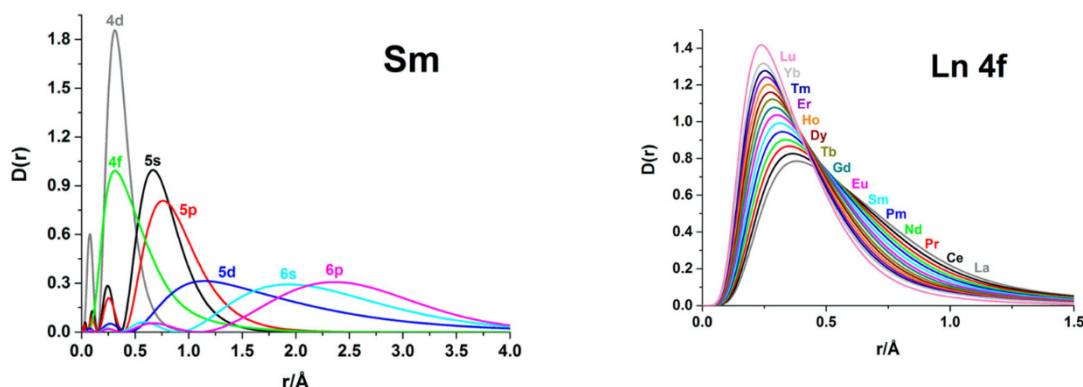

Fig. 2. Radial density distribution function D(r) = r²R² of rare earth metals[37]

Rare-earth borides are important materials with unique magnetic, thermoelectric, and superhard properties[38]. However, relatively less attention was paid to the rare-earth boron clusters. In order to explore their chemical bonding, electronic structures and spectroscopic properties, we have performed a series of joint PES and quantum chemical theoretical studies on lanthanide boride clusters, which reveals interesting geometric structures such as planar[39, 40], half-sandwich[41], and inverse sandwich complexes[42-44]. The inverse sandwich structures, adopting the M···L···M motif (M is the metal and L represents the ligand), have been widely known for the transition metals and actinide elements protected by organic hydrocarbon ring ligands[45-50]. The interlayer ligands are mostly aromatic rings, which can form stable chemical bonds to metals on both faces via its delocalized ligand group orbitals. However, such structures have seldom been observed in boride clusters before. In this paper, we provide an overview on the recent results of lanthanide-boron inverse-sandwich compounds that feature a new class of clusters with unprecedented structures and chemical bonding patterns.

2 PROGRESS OF RESEARCH

As mentioned above, B$_7$, B$_8$ and B$_9$ rings have the suitable size to stably match with two lanthanide atoms. Recently, joint theoretical and PES studies have verified the existence of

these $Ln_2B_n^-$ (n = 7,8,9) species[42, 43]. Local coordinate system (LCS) analysis is an effective tool to analyze the orbital interactions between metal atom and ligands, especially for molecules with high symmetry[24, 51]. Fig. 3 presents the LCS analyses of B_n (n = 7, 8, 9) clusters to investigate how they interact with the two lanthanide elements. These rings have $4n$ 2s/2p valence orbitals which can be divided into four categories according to the different spatial orientation of the orbitals, classified into σ_s, $\sigma(t)_p$, $\sigma(r)_p$, and π_p orbitals, where "t" and "r" represent "tangential" and "radial" interaction, and s and p denote the B 2s and 2p orbitals, respectively. Number in the subscript corresponds to the number of the nodal plane (Fig. 3).

The BB bonds in the boron rings are found to arise from the occupied σ_s and $\sigma(t)_p$ orbitals that are bonding or non-bonding on the basis of a tight-binding Hückel-type consideration. The covalent interaction between BB atoms of the ring is rather strong so that the splitting of the occupied and unoccupied regions in σ_s and $\sigma(t)_p$ groups are much larger than that in the delocalized $\sigma(r)_p$, and π_p orbitals, which dominantly constitute the interaction between lanthanide metals and boron rings. When forming the Ln_2B_n inverse sandwich complexes, two Ln atoms donate four electrons to the boron ring, giving rise to the fully occupied σ_{r1} orbitals that are doubly degenerate. It is interesting to note that similar to the C_nH_n rings that fulfill the ($4n$ + 2) π-electron rule for forming ring ligands with different charges, $C_3H_3^+$, $C_4H_4^{2-}$, $C_5H_5^-$, C_6H_6 (or $C_6H_6^{4-}$), $C_7H_7^{3-}$ ($C_7H_7^+$), and $C_8H_8^{2-}$[52], the boron ring ligands B_6^{6-}, B_7^{5-}, B_8^{4-}, B_9^{3-} and B_{10}^{2-} are perfect for closed shells. In other words, one can view these pure boron ring ligands as hexavalent, pentavalent, tetravalent, trivalent, and divalent, respectively. These B_n^{x-} ligands often have high-lying valence bonding orbitals because of the low electronegativity of boron, which make them suitable for matching energetically with lanthanide 5d orbitals. Besides, they can force metal atoms to form uncommon oxidation states, as in the case of Pr(I) and Pr(II)[39].
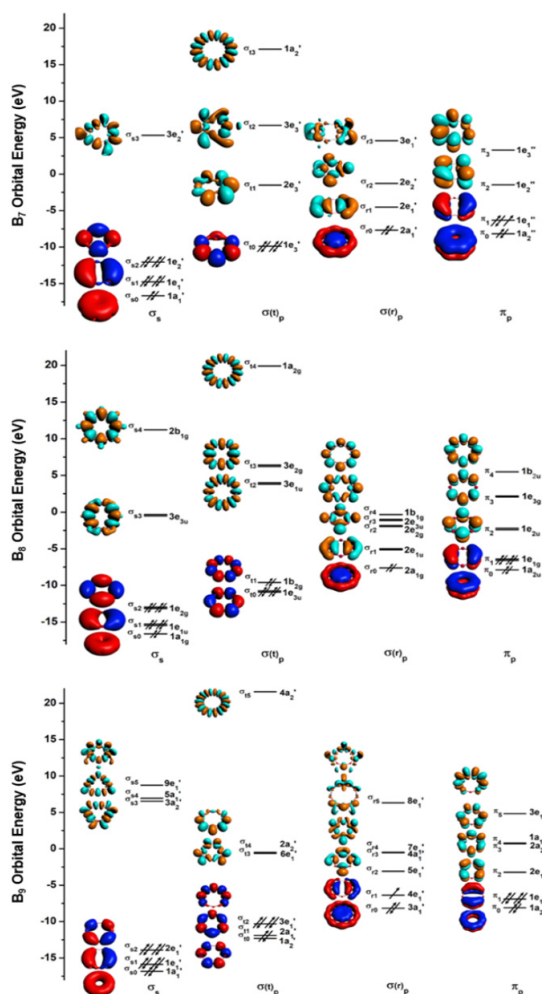

Fig. 3. Molecular orbital (MO) energy level of B_n (n = 7, 8, 9) in local coordinate system (LCS).

"t" and "r" represent "tangential" and "radial" orbitals, respectively[43]

We performed canonical molecular orbital (CMO) analysis for La_2B_8 inverse sandwich clusters as an example to figure out the interactions between two La atoms and the B_8 ring, as shown in Fig. 4. The unoccupied π_2 orbital from B_n is significantly stabilized by a symmetry-matching La···La d-δ_u type of orbital, which leads to the formation of the unique (d-p)δ chemical bonding. This (d-p)δ interaction has an enormous contribution ($La_2B_7^-$: 6.9%, $La_2B_8^-$: 16.9%, $La_2B_9^-$: 42.4%) to the total orbital interaction. The only difference between the neutral and anion species originates from the occupation number of electrons on such (d-p)δ molecular orbital, where there is slight Jahn-Teller effect in the $La_2B_8^-$ system due to degeneracy. In the Ln_2B_n sandwich clusters, LUMOs are primarily composed of Ln $6s$ orbital displaying a huge gap from the HOMOs with (d-p)δ bonding, indicating the overwhelming stability of the rare-earth inverse sandwich compounds.

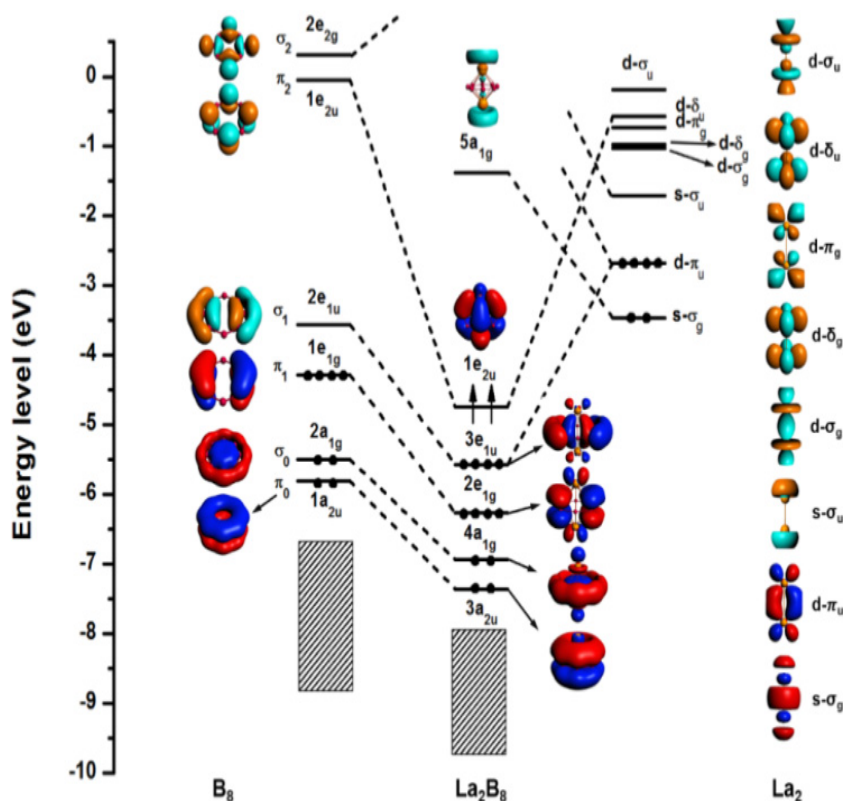**Fig. 4.** Chemical bonding interactions between the La···La and B_8 fragments in D_{8h} La_2B_8 at the level of PBE0/TZP[42]

The semi-localized natural bonding orbital approach, AdNDP (Adaptive Natural Density Partitioning method), is another powerful tool to understand the chemical bonding in $Ln_2B_n^-$ inverse sandwich clusters[53]. The AdNDP analyses yield both localized and semi-localized multi-center bonds, providing a chemically intuitive bonding picture for complicated molecular systems that cannot be described with the two-electron, two center (2c-2e) bonding formalism. As shown in Fig. 5, the n 2c-2e σ bonds constitute the frame of B_n^- rings, and all other bonds are more or less delocalized due to the electron deficiency of boron. The delocalized n-center two-electron (nc-2e) σ and π bonds give rise to double aromaticity features for the inverse sandwich clusters, each satisfying the $(4n + 2)$ Hückel rule. The (d-p)δ bonding in $Ln_2B_n^-$ ($n = 7 \sim 9$) are different. The $Ln_2B_9^-$ inverse sandwich has two full (d-p)δ bonds, whereas the $Ln_2B_7^-$ and $Ln_2B_8^-$ inverse sandwich clusters only possess partial (d-p)δ bonds, which renders extraordinary stability for the $Ln_2B_9^-$ cluster.
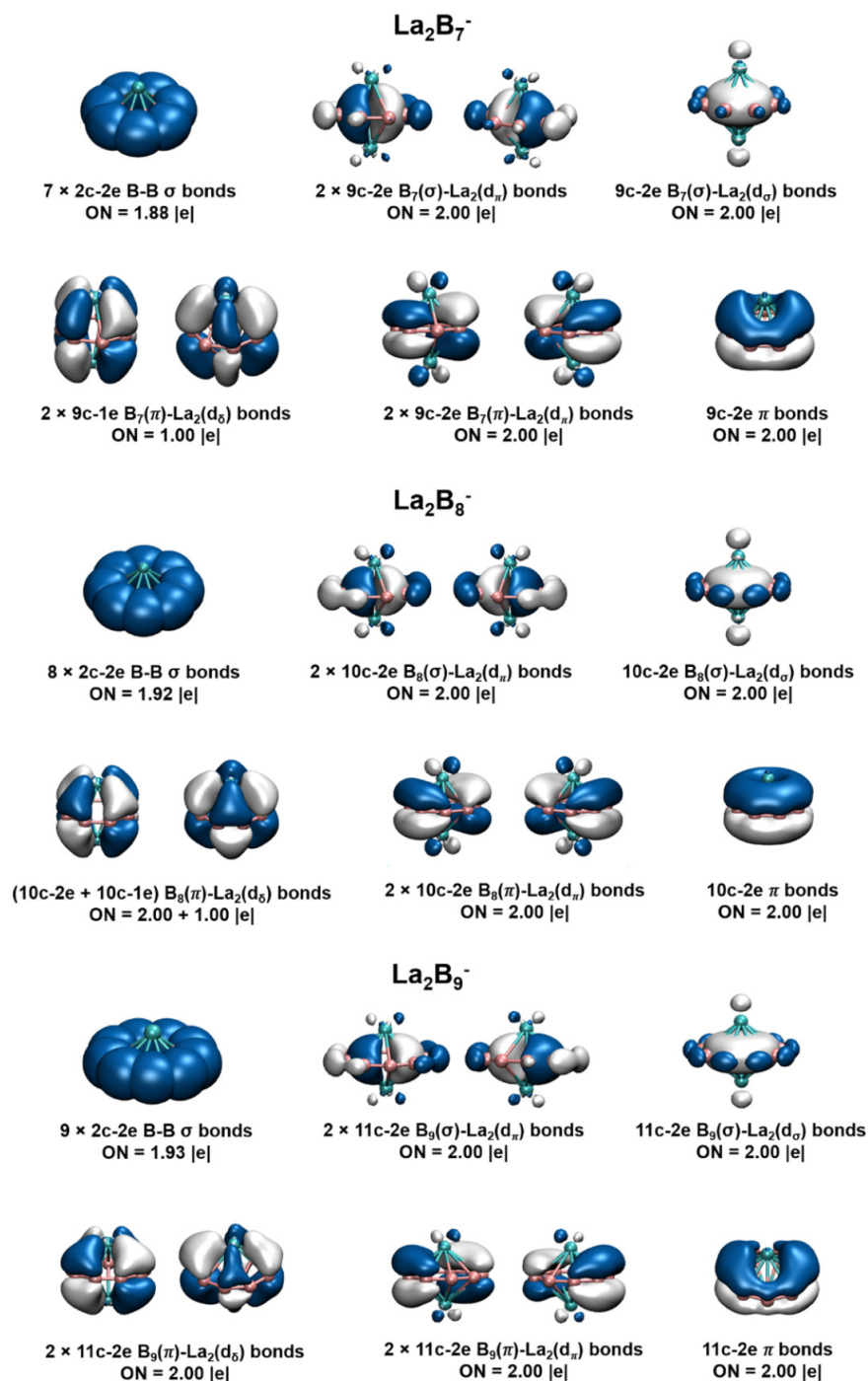
La₂B₇⁻

7 × 2c-2e B-B σ bonds
ON = 1.88 |e|

2 × 9c-2e B₇(σ)-La₂(dπ) bonds
ON = 2.00 |e|

9c-2e B₇(σ)-La₂(d_σ) bonds
ON = 2.00 |e|

2 × 9c-1e B₇(π)-La₂(d_δ) bonds
ON = 1.00 |e|

2 × 9c-2e B₇(π)-La₂(dπ) bonds
ON = 2.00 |e|

9c-2e π bonds
ON = 2.00 |e|

La₂B₈⁻

8 × 2c-2e B-B σ bonds
ON = 1.92 |e|

2 × 10c-2e B₈(σ)-La₂(dπ) bonds
ON = 2.00 |e|

10c-2e B₈(σ)-La₂(d_σ) bonds
ON = 2.00 |e|

(10c-2e + 10c-1e) B₈(π)-La₂(d_δ) bonds
ON = 2.00 + 1.00 |e|

2 × 10c-2e B₈(π)-La₂(dπ) bonds
ON = 2.00 |e|

10c-2e π bonds
ON = 2.00 |e|

La₂B₉⁻

9 × 2c-2e B-B σ bonds
ON = 1.93 |e|

2 × 11c-2e B₉(σ)-La₂(dπ) bonds
ON = 2.00 |e|

11c-2e B₉(σ)-La₂(d_σ) bonds
ON = 2.00 |e|

2 × 11c-2e B₉(π)-La₂(d_δ) bonds
ON = 2.00 |e|

2 × 11c-2e B₉(π)-La₂(dπ) bonds
ON = 2.00 |e|

11c-2e π bonds
ON = 2.00 |e|

Fig. 5. Localized and semi-localized MOs from AdNDP analysis of MB_xM (x = 7, 8, 9)[43]

The La_2B_n species demonstrates magnetic properties because of the partially occupied (d-p)δ orbitals. Other Ln_2B_n inverse sandwich clusters with 4f electrons have more complicated magnetic coupling character due to more local 4f electrons on each Ln center, such as the Pr_2B_8 complex[54]. The multi-configurational wavefunction dominantly comes from different 4f-shell occupancy, but the general bonding pattern in Pr_2B_8 remains the same as that in La_2B_8. Theoretical calculations obtained from *ab initio* CASPT2 method found that electronic state with ferromagnetic coupling is at least 8.73 kcal/mol lower in energy than that of the antiferromagnetic case. Due to the similar patterns of photoelectron spectra and chemical bonding for $La_2B_8^-$, $Pr_2B_8^-$ and $Tb_2B_8^-$, all Ln_2B_8 complexes are assumed to have similar structures and bonding, providing opportunities to design highly magnetic Ln_2B_8 sandwich complexes, as well as one-dimensional (1D) magnetic nanowires.
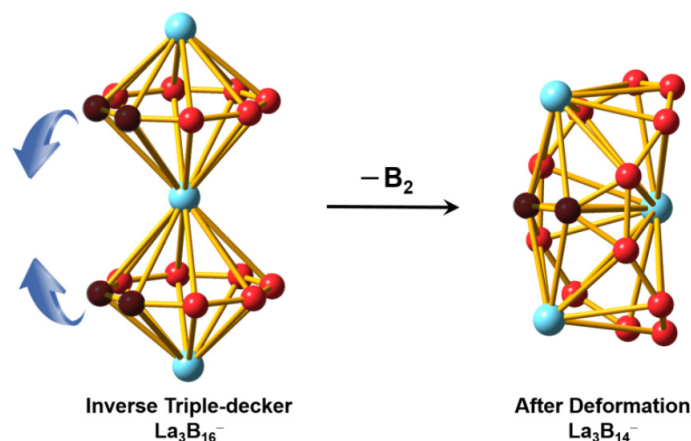
Fig. 6.　Schematic illustration of the transformation from a perfect linear inverse triple-decker,
La···B$_8$···La···B$_8$···La, the bent triple-decker of La$_3$B$_{14}^-$, with two conjoined B$_8$ rings by sharing a B$_2$ unit

As shown in Fig. 6, combined PES and theoretical studies have revealed that the global-minimum-energy structure of La$_3$B$_{14}^-$ anion cluster[44] has closed-shell configuration with a C_{2v} symmetry, which can be viewed as an "inverse triple-decker" with two conjoined B$_8$ rings sharing a BB unit due to strong inter-layer BB bonding. Theoretically, the oligomers formed by elongation of such deformed inverse triple-decker are also found to be stable. Presumably, infini-tely long 1D lanthanide-boron nanostructures consisting of conjoint B$_8$ rings are viable or could be found in crystalline lattices of new lanthanide boride materials.
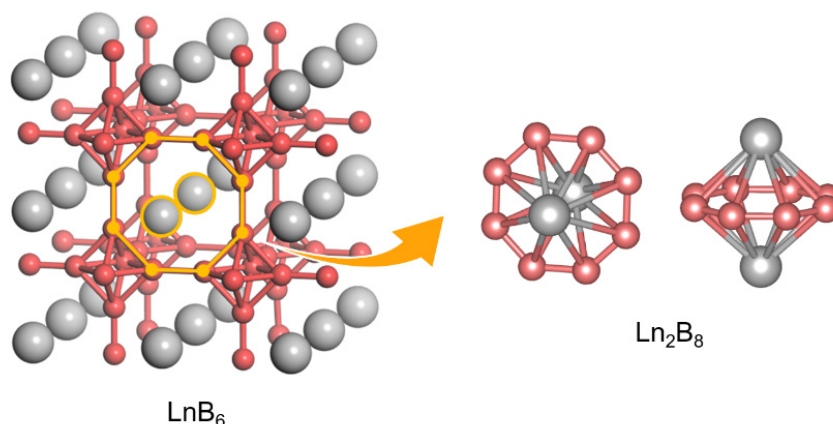

Fig. 7.　Connection of Ln$_2$B$_8$ sandwich cluster with structural unit of solid LnB$_6$ material.
Red and grey atoms correspond to B and La, respectively[55]

Another interesting aspect is that the D_{8h}-[LnB$_8$Ln] gaseous inverse sandwich cluster is reminiscent of the structural motif in the popular material of LnB$_6$, as shown in Fig. 7. This structural connection is interesting as it well establishes a relationship between gaseous clusters and solid phase materials[55]. And in fact, the bulk crystal structure can be viewed through a different angle using the Ln$_2$B$_8$ clusters. The crystal structure of LnB$_6$ has simple cubic space group: Pm-$3m$, with B$_6$-octahedra in body-centered positions and La atoms at the corners of the unit cell. From another perspective, we can take Ln$_2$B$_8$ as a repeat unit extending indefinitely in the three-dimensional(3D) space in three perpendicular directions, as shown in Fig. 6. Each B atom in Ln$_2$B$_8$ region belongs to eight vertexes in four B$_6$-octahedra in the same plane. Taking PrB$_6$ solid material as an example, the bond lengths between two neighboring B atoms are measured to be 1.708 and 1.706 Å for internal and external octahedral respectively, and the distance between two Pr atoms in one unit is 4.121 Å, which are longer than those in the Pr$_2$B$_8$ cluster because of different bonding conditions in periodic constructions[56].
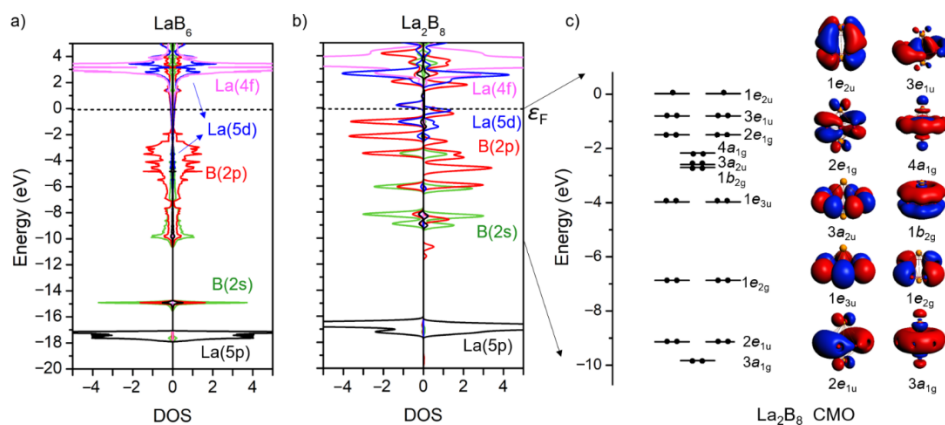
Fig. 8. a) and b) Density of states (DOS) for both solid LaB$_6$ and gaseous La$_2$B$_8$ with majority (right) and minority (left) spins. c) MO levels and the 3D orbital contours of La$_2$B$_8$

In addition, the two systems resemble each other in terms of electronic structure, as shown in Fig. 8. The orbital interaction between La 5d and B 2p is the primary contribution to the La-B bonding, but Ln$_2$B$_8$ inverse sandwich clusters demonstrate increased covalent character despite the major bonding between Ln and B$_8$ cluster is ionic in nature. The curves in proximity to the Fermi level look spiky or even discrete for isolated La$_2$B$_8$ but continuous or broadened for solid-state LaB$_6$.

The Ln$_2$B$_8$ clusters provide a new perspective to view the bulk LnB$_6$ crystal structures as repeating units of clusters in three perpendicular directions. The similarity between clusters and crystals is unrecognized in such compounds. Since the bulk LnB$_6$ represents a series of important magnetic, electric and superconducting materials, exploring the bonding and electronic structures of clusters provides us a new avenue to understand the bonding and physical mechanisms for these unique properties via establishing a link by repetitions of cluster structures.

3 CONCLUSION AND PERSPECTIVE

In this article, we have summarized our recent research progresses on a series of rare-earth boron inverse-sandwich clusters Ln$_2$B$_n$ ($n = 7 \sim 9$), which provide a new class of cluster complexes with unique geometric structures, interesting bonding mechanism, and magnetic properties. Two lanthanide elements interact with the boron rings via lanthanide 5d orbitals and 2s/2p delocalized group orbitals from B$_n$, giving rise to multi-center bonding and aromaticity to cause the structures to be stable. Especially noteworthy is the rare (d-p)δ type bonding in this kind of clusters, which renders extraordinary stability and contributes unexpectedly

to the whole orbital interactions. The electron-deficiency features of boron elements and the more extended 2s/2p valence orbitals make the B$_n$ rings better ligands for interacting with lanthanides than the C$_n$H$_n$ hydrocarbon rings[4].

Especially noteworthy is the finding that the highly symmetric Ln$_2$B$_8$ clusters can be viewed as a structural unit to build well-known LnB$_6$ solid materials. The concept of structural unit assembly into cluster compounds has been in place for a long time, as was initially proposed by Jia-Xi Lu et al. in the unit construction approach to the rational synthesis of transition-metal cubane-like clusters[57]. The connection of rare-earth boride clusters and the relevant solid materials provides a new insight in establishing relationships between gaseous phase clusters and cluster-assembled solid phase materials. Further study of the relationship of cluster structural unit and cluster-assembled materials of rare-earth borides would be interesting for further research in this area.

Since lanthanides have different unpaired 4f-electrons and high spins, these Ln-B clusters and solids with a variety of possible spin couplings can form a basis for exploring innovated materials for applications in electronic, magnetic, optical, and thermoelectric fields. The multifaceted and novel magnetic features of these compounds may find future applications in electronics. Because of the high-lying yet radially extended 5d orbitals and low-lying but core-like 4f orbitals, the lanthanides are unique in the periodic table[58]. The unusual behavior of lanthanides in forming borides with significantly different properties from those of transition metals can be utilized to discover new cluster molecules and innovative materials in f-element chemistry. We are working on further exploring the solid-state materials of rare-earth metal boron clusters to provide understanding of such novel properties of the solid materials.

REFERENCES

(1)   Tang, A. C.; Li, Q. S.; Liu, C. W.; Li, J. Symmetrical clusters of carbon and boron. *Chem. Phy. Lett.* **1993**, 5-6, 465-469.

(2)   Zhai, H. J.; Kiran, B.; Li, J.; Wang, L. S. Hydrocarbon analogues of boron clusters-planarity, aromaticity and antiaromaticity. *Nat. Mater.* **2003**, 2, 827–833.

(3)   Alexandrova, A. N.; Boldyrev, A. I.; Zhai, H. J.; Wang, L. S.; Steiner, E.; Fowler, P. W. Structure and bonding in B_6^- and B_6: planarity and antiaromaticity. *J. Phys. Chem. A* **2003**, 9, 1359–1369.

(4)   Li, W.; Hu, H.; Zhao, Y.; Chen, X.; Chen, T.; Jian, T.; Wang, L.; Li, J. Recent progress on the investigations of boron clusters and boronbased materials(I): borophene. *Sci. Sinica Chim.* **2018**, 2, 98–107.

(5)   Li, W. L.; Chen, X.; Jian, T.; Chen, T. T.; Li, J.; Wang, L. S. From planar boron clusters to borophenes and metalloborophenes. *Nat. Rev. Chem.* **2017**, 1, 71.

(6)   Sergeeva, A. P.; Popov, I. A.; Piazza, Z. A.; Li, W. L.; Romanescu, C.; Wang, L. S.; Boldyrev, A. I. Understanding boron through size-selected clusters: structure, chemical bonding, and fluxionality. *Acc. Chem. Res.* **2014**, 4, 1349–1358.

(7)   Boldyrev, A. I.; Wang, L. S. Beyond organic chemistry: aromaticity in atomic clusters. *Phys. Chem. Chem. Phys.* **2016**, 17, 11589-11605.

(8)   Wang, L. S. Photoelectron spectroscopy of size-selected boron clusters: from planar structures to borophenes and borospherenes. *Int. Rev. Phys. Chem.* **2016**, 1, 69–142.

(9)   Bai, H.; Chen, T. T.; Chen, Q.; Zhao, X. Y.; Zhang, Y. Y.; Chen, W. J.; Li, W. L.; Cheung, L. F.; Bai, B.; Cavanagh, J.; Huang, W.; Li, S. D.; Li, J.; Wang, L. S. Planar B_{41}^- and B_{42}^- clusters with double-hexagonal vacancies. *Nanoscale* **2019**, 48, 23286–23295.

(10) Chen, Q.; Chen, T. T.; Li, H. R.; Zhao, X. Y.; Chen, W. J.; Zhai, H. J.; Li, S. D.; Wang, L. S. B_{31}^- and B_{32}^-: chiral quasi-planar boron clusters. *Nanoscale* **2019**, 19, 9698–9704.

(11) Li, W. L.; Chen, Q.; Tian, W. J.; Bai, H.; Zhao, Y. F.; Hu, H. S.; Li, J.; Zhai, H. J.; Li, S. D.; Wang, L. S. The B_{35} cluster with a double-hexagonal vacancy: a new and more flexible structural motif for borophene. *J. Am. Chem. Soc.* **2014**, 35, 12257–12260.

(12) Piazza, Z. A.; Hu, H. S.; Li, W. L.; Zhao, Y. F.; Li, J.; Wang, L. S. Planar hexagonal B_{36} as a potential basis for extended single-atom layer boron sheets. *Nat. Commun.* **2014**, 5, 3113.

(13) Mannix, A. J.; Zhou, X. F.; Kiraly, B.; Wood, J. D.; Alducin, D.; Myers, B. D.; Liu, X.; Fisher, B. L.; Santiago, U.; Guest, J. R.; Yacaman, M. J.; Ponce, A.; Oganov, A. R.; Hersam, M. C.; Guisinger, N. P. Synthesis of borophenes: Anisotropic, two-dimensional boron polymorphs. *Science* **2015**, 6267, 1513–1516.

(14) Feng, B.; Zhang, J.; Zhong, Q.; Li, W.; Li, S.; Li, H.; Cheng, P.; Meng, S.; Chen, L.; Wu, K. Experimental realization of two-dimensional boron sheets. *Nat. Chem.* **2016**, 6, 564–569.

(15) Zhai, H. J.; Zhao, Y. F.; Li, W. L.; Chen, Q.; Bai, H.; Hu, H. S.; Piazza, Z. A.; Tian, W. J.; Lu, H. G.; Wu, Y. B.; Mu, Y. W.; Wei, G. F.; Liu, Z. P.; Li, J.; Li, S. D.; Wang, L. S. Observation of an all-boron fullerene. *Nat. Chem.* **2014**, 8, 727–731.

(16) Chen, Q.; Li, W. L.; Zhao, Y. F.; Zhang, S. Y.; Hu, H. S.; Bai, H.; Li, H. R.; Tian, W. J.; Lu, H. G.; Zhai, H. J.; Li, S. D.; Li, J.; Wang, L. S. Experimental and theoretical evidence of an axially chiral borospherene. *ACS Nano.* **2015**, 1, 754–760.

(17) Jian, T.; Chen, X.; Li, S. D.; Boldyrev, A. I.; Li, J.; Wang, L. S. Probing the structures and bonding of size-selected boron and doped-boron clusters. *Chem. Soc. Rev.* **2019**, 13, 3550–3591.

(18) Zhai, H. J.; Wang, L. S.; Alexandrova, A. N.; Boldyrev, A. I. Electronic structure and chemical bonding of B_5^- and B_5 by photoelectron spectroscopy and *ab initio* calculations. *J. Chem. Phys.* **2002**, 17, 7917–7924.

(19) Alexandrova, A. N.; Boldyrev, A. I.; Zhai, H. J.; Wang, L.S.; Steiner, E.; Fowler, P. W. Structure and bonding in B_6^- and B_6: planarity and antiaromaticity. *J. Phys. Chem. A*. **2003**, 9, 1359–1369.

(20) Zhai, H. J.; Alexandrova, A. N.; Birch, K. A.; Boldyrev, A. I.; Wang, L. S. Hepta‐and octacoordinate boron in molecular wheels of eight‐and nine‐atom boron clusters: observation and confirmation. *Angew. Chem. Int. Ed.* **2003**, 48, 6004–6008.

(21) Li, W. L.; Zhao, Y. F.; Hu, H. S.; Li, J.; Wang, L. S. [B_{30}]: a quasiplanar chiral boron cluster". *Angew. Chem. Int. Ed.* **2014**, 53, 5540–5545.

(22) Zhai, H. J.; Wang, L. S.; Alexandrova, A. N.; Boldyrev, A. I.; Zakrzewski, V. G. Photoelectron spectroscopy and *ab initio* study of B_3^- and B_4^- anions and their neutrals. *J. Phys. Chem. A* **2003**, 44, 9319–9328.

(23) Alexandrova, A. N.; Boldyrev, A. I.; Zhai, H. J.; Wang, L. S. Electronic structure, isomerism, and chemical bonding in B_7^- and B_7. *J. Phys. Chem. A* **2004**, 16, 3509–3517.

(24) Dennington, R.; Keith, T.; Millam, J. GaussView, version 4.1; Semichem, Inc., Shawnee Mission, KS **2007**.

(25) Chung, H. Y.; Weinberger, M. B.; Levine, J. B.; Kavner, A.; Yang, J. M.; Tolbert, S. H.; Kaner, R. B. Synthesis of ultra-incompressible superhard rhenium diboride at ambient pressure. *Science* **2007**, 5823, 436–439.

(26) Carenco, S.; Portehault, D.; Boissière, C.; Mézailles, N.; Sanchez, C. Nanoscaled metal borides and phosphides: recent developments and perspectives. *Chem. Rev.* **2013**, 10, 7981–8065.

(27) Sussardi, A.; Tanaka, T.; Khan, A. U.; Schlapbach, L.; Mori, T. Enhanced thermoelectric properties of samarium boride. *J. Materiomics* **2015**, 3, 196–204.

(28) Scheifers, J. P.; Zhang, Y.; Fokwa, B. P. T. Boron: enabling exciting metal-rich structures and magnetic properties. *Acc. Chem. Res.* **2017**, 9, 2317–2325.

(29) Akopov, G.; Yeung, M. T.; Kaner, R. B. Rediscovering the crystal chemistry of borides. *Adv. Mater.* **2017**, 21, 1604506.

(30) Paderno, Y. B.; Pokrzywnicki, S.; Staliński, B. Magnetic properties of some rare earth hexaborides. *Phys. Status Solidi b-Basic Res.* **1967**, 1, K73–K76.

(31) Geballe, T. H.; Matthias, B. T.; Andres, K.; Maita, J. P.; Cooper, A. S.; Corenzwit, E. Magnetic ordering in the rare-earth hexaborides. *Science* **1968**, 3835, 1443–1444.

(32) Zhitomirsky, M. E.; Rice, T. M.; Anisimov, V. I. Ferromagnetism in the hexaborides. *Nature* **1999**, 6759, 251–253.

(33) Mori, T. Thermoelectric and magnetic properties of rare earth borides: boron cluster and layered compounds. *J. Solid State Chem.* **2019**, 70–82.

(34) Pyykkö, P. Dirac-Fock One-centre calculations part 8. The$^1\Sigma$ states of ScH, YH, LaH, AcH, TmH, LuH and LrH. *Physica Scripta* **1979**, 5-6, 647–651.

(35) Kaupp, M. The role of radial nodes of atomic orbitals for chemical bonding and the periodic table. *J. Comput. Chem.* **2007**, 1, 320–325.

(36) Tang, Y.; Zhao, S.; Long, B.; Liu, J. C.; Li, J. On the nature of support effects of metal dioxides MO_2 (M = Ti, Zr, Hf, Ce, Th) in single-atom gold catalysts: importance of quantum primogenic effect. *J. Phys. Chem. C* **2016**, 31, 17514–17526.

(37) Lu, J. B.; Cantu, D. C.; Nguyen, M. T.; Li, J.; Glezakou, V. A.; Rousseau, R. Norm-conserving pseudopotentials and basis sets to explore lanthanide chemistry in complex environments. *J. Chem. Theory Comput.* **2019**, 11, 5987–5997.

(38) Takao Mori: *encyclopedia of inorganic and bioinorganic chemistry*. John Wiley & Sons, Ltd: Online **2012**, DOI: 10.1002/9781119951438.eibc2028.

(39) Chen, X.; Chen, T. T.; Li, W. L.; Lu, J. B.; Zhao, L. J.; Jian, T.; Hu, H. S.; Wang, L. S.; Li, J. Lanthanides with unusually low oxidation states in the PrB₃⁻ and PrB₄⁻ boride clusters. *Inorg. Chem.* **2019**, 1, 411–418.

(40) Robinson, P. J.; Zhang, X.; McQueen, T.; Bowen, K. H.; Alexandrova, A. N. SmB₆ cluster anion: covalency involving *f* orbitals. *J. Phys. Chem. A* **2017**, 8, 1849–1854.

(41) Chen, T. T.; Li, W. L.; Jian, T.; Chen, X.; Li, J.; Wang, L. S. PrB₇⁻: a praseodymium-doped boron cluster with a Pr^{II} center coordinated by a doubly aromatic planar η^7-B₇³⁻ ligand. *Angew. Chem. Int. Ed.* **2017**, 24, 6916–6920.

(42) Li, W. L.; Chen, T. T.; Xing, D. H.; Chen, X.; Li, J.; Wang, L. S. Observation of highly stable and symmetric lanthanide octa-boron inverse sandwich complexes. *Proc. Natl. Acad. Sci. USA* **2018**, 30, E6972–E6977.

(43) Chen, T. T.; Li, W. L.; Li, J.; Wang, L. S. [La(η^x-B$_x$)La]⁻ (x = 7∼9): a new class of inverse sandwich complexes. *Chem. Sci.* **2019**, 8, 2534–2542.

(44) Chen, T. T.; Li, W. L.; Chen, W. J.; Li, J.; Wang, L. S. La₃B₁₄⁻: an inverse triple-decker lanthanide boron cluster. *Chem. Commun.* **2019**, 54, 7864–7867.

(45) Duff, A. W.; Jonas, K.; Goddard, R.; Kraus, H. J. and Krueger, C. The first triple-decker sandwich with a bridging benzene ring. *J. Am. Chem. Soc.* **1983**, 5479–5480.

(46) Schier, A.; Wallis, J. M.; Müller, G.; Schmidbaur, H. [C₆H₃(CH₃)₃][BiCl₃] and [C₆(CH₃)₆][BiCl₃]₂, arene complexes of bismuth with half-sandwich and "inverted" sandwich structures. *Angew. Chem. Int. Ed. Engl.* **1986**, 8, 757–759.

(47) Streitwieser, A.; Smith, K. A. Inverse sandwich compounds. *J. Mol. Struct. Theochem.* **1988**, 259–265.

(48) Arliguie, T.; Lance, M.; Nierlich, M.; Vigner, J.; Ephritikhine, M. Inverse cycloheptatrienyl sandwich complexes. Crystal structure of [U(BH₄)₂(OC₄H₈)₅][(BH₄)₃U(μ-η^7,η^7-C₇H₇)U(BH₄)₃]. *J. Chem. Soc., Chem. Commun.* **1994**, 7, 847–848.

(49) Krieck, S.; Görls, H.; Yu, L.; Reiher, M.; Westerhausen, M. Stable "inverse" sandwich complex with unprecedented organocalcium(I): crystal structures of [(thf)₂Mg(Br)-C₆H₂-2,4,6-Ph₃] and [(thf)₃Ca{μ-C₆H₃-1,3,5-Ph₃}Ca(thf)₃]. *J. Am. Chem. Soc.* **2009**, 8, 2977–2985.

(50) Diaconescu, P. L.; Arnold, P. L.; Baker, T. A.; Mindiola, D. J.; Cummins, C. C. Arene-bridged diuranium complexes: inverted sandwiches supported by δ backbonding. *J. Am. Chem. Soc.* **2000**, 25, 6108–6109.

(51) Li, J.; Liu, C. W.; Lu, J. X. Quantum chemical studies on the bonding characteristics of some M_3X_4 transition-metal halogenide clusters. *J. Cluster Sci.* 1994, 505–521.

(52) Li, J.; Liu, C. W.; Lu, J. X. Abinitio studies on the electronic-structures of certain 10-π-electron 6-membered ring compounds. *J. Mol. Struct. Theochem.* **1993**, 2-3, 223–231.

(53) Zubarev, D. Y.; Boldyrev, A. I. Developing paradigms of chemical bonding: adaptive natural density partitioning. *Phys. Chem. Chem. Phys.* **2008**, 34, 5207–5217.

(54) Li, W. L.; Chen, T. T.; Xing, D. H.; Chen, X.; Li, J.; Wang, L. S. Observation of highly stable and symmetric lanthanide octa-boron inverse sandwich complexes. *Proc. Natl. Acad. Sci. USA* **2018**, 30, E6972–E6977.

(55) Li, W. L.; Ertural, C.; Bogdanovski, D.; Li, J.; Dronskowski, R. Chemical bonding of crystalline LnB_6 (Ln = LaLu) and its relationship with Ln_2B_8 gas-phase complexes. *Inorg. Chem.* **2018**, 20, 12999–13008.

(56) Wyckoff, R. W. G.: *The Structure of Crystals.* Chemical Catalog Company **1924**.

(57) Lu, J. X.; Zhuang, B. T. A unit conrstruction approach to the rational synthese of transition metal cabane-lake clusters by the use of reactive fragments as buioding blocks. *Chin. J. Struct. Chem.* **1989**, 04, 233–248.

(58) Cao, C. S.; Hu, H. S.; Li, J.; Schwarz, W. H. E. Physical origin of chemical periodicities in the system of elements. *Pure and Appl. Chem.* **2019**, 12, 1969–1999.